

The coordinate regulation of pharyngeal development in *C. elegans* by *lin-35/Rb*, *pha-1*, and *ubc-18*

David S. Fay,^{a,*} Xiaohui Qiu,^a Edward Large,^a Christopher P. Smith,^a
Susan Mango,^b and Bethany L. Johanson^a

^aDepartment of Molecular Biology, College of Agriculture, University of Wyoming, Laramie, WY 82071-3944, USA

^bHuntsman Cancer Institute Center for Children, University of Utah 2000, Circle of Hope, Salt Lake City, UT 84112, USA

Received for publication 20 March 2004, accepted 20 March 2004

Available online 27 April 2004

Abstract

Organ development is a complex process involving the coordination of cell proliferation, differentiation, and morphogenetic events. Using a screen to identify genes that function coordinately with *lin-35/Rb* during animal development, we have isolated a weak loss-of-function (LOF) mutation in *pha-1*. *lin-35; pha-1* double mutants are defective at an early step in pharyngeal morphogenesis leading to an abnormal pharyngeal architecture. *pha-1* is also synthetically lethal with other class B synthetic multivulval (SynMuv) genes including the *C. elegans* E2F homolog, *efl-1*. Reporter analyses indicate that *pha-1* is broadly expressed during embryonic development and that its functions reside in the cytoplasm. We also provide genetic and phenotypic evidence to support the model that PHA-1, a novel protein, and UBC-18, a ubiquitin-conjugating enzyme that we have previously shown to function with *lin-35* during pharyngeal development, act in parallel pathways to regulate the activity of a common cellular target.

© 2004 Elsevier Inc. All rights reserved.

Keywords: *lin-35*; Retinoblastoma; *pha-1*; Pharynx; *ubc-18*; Genetic redundancy; Organogenesis

Introduction

Studies over the past 30 years have revealed the tremendous complexity in the genetic and biochemical mechanisms that control organismal development. It is now evident that in addition to being controlled by large numbers of gene products, most developmental processes are regulated by intricate networks of parallel and intersecting pathways. This facet of developmental control is underscored by the widespread phenomenon of genetic redundancy—the observation that two or more genes may perform similar or complementary biological functions. Because of such overlap, individual mutations in many genes may have little or no effect on the developmental program of the organism. In contrast, compound mutations in two or more “redundant” genes may produce a clear-cut

“synthetic” phenotype. Although the full extent of genetic redundancy is not known for most organisms, studies from yeast and *C. elegans* indicate that a substantial fraction of genes (perhaps the majority) direct functions that are at least partially, if not largely, redundant with the activities of other genes (Fraser et al., 2000; Hodgkin, 2001; Kamath and Ahringer, 2003; Smith et al., 1996; Tong et al., 2004; Winzeler et al., 1999). This unavoidable aspect of biology presents a continuing conceptual and technical challenge to researchers seeking to understand the complex means by which cellular and developmental processes are controlled.

One of the best-studied examples of genetic redundancy in a multicellular organism is the synthetic multivulval (SynMuv) mutants of *C. elegans* (Ferguson and Horvitz, 1989). Most SynMuv genes belong exclusively to one of two classes, A or B. In general, the isolated class A and B mutations have little or no phenotype either as single mutants or when paired with other mutations from the same class. However, animals containing compound mutations in genes from both classes display a highly penetrant Muv phenotype, indicating that class A and B genes are genetically redundant

* Corresponding author. Department of Molecular Biology, Dept. 3944, College of Agriculture, University of Wyoming, 1000 East University Avenue, Laramie, WY 82071-3944. Fax: +1-307-766-5098.

E-mail address: davidfay@uwyo.edu (D.S. Fay).

(reviewed by Fay and Han, 2000). Although the molecular functions of the class A genes are largely unknown, many class B genes encode homologs of well-studied transcriptional regulators. These include histone deacetylase (Lu and Horvitz, 1998); several nucleosome remodeling (NURD) components (Solari and Ahringer, 2000; von Zelewsky et al., 2000); a heterochromatin protein 1 homolog, *hpl-2* (Couteau et al., 2002); *efl-1*, a homolog of mammalian E2F (Ceol and Horvitz, 2001); and the *C. elegans* Retinoblastoma protein (Rb) homolog, *lin-35* (Lu and Horvitz, 1998).

A large body of work, mostly from mammalian systems, has generated a model in which Rb, when bound to E2F, recruits factors that can mediate transcriptional repression (reviewed by Harbour and Dean, 2000; Kaelin, 1999; Morris and Dyson, 2001). These factors include histone deacetylase (Brehm et al., 1998; Luo et al., 1998; Magnaghi-Jaulin et al., 1998), NURD complex components (Dunaief et al., 1994; Strober et al., 1996; Zhang et al., 2000), and proteins associated with heterochromatin formation and maintenance (Dahiya et al., 2001; Narita et al., 2003; Nielsen et al., 2001). This leads to localized changes in chromatin structure and the down-regulation of E2F target genes, many of which include factors required for the initiation and execution of S phase and DNA replication (e.g., DeGregori et al., 1995; Dou et al., 1994).

Through screens for mutations that show synthetic phenotypes with *lin-35*, we have previously shown that *fzr-1*, a conserved component of the APC ubiquitin–ligase complex, functions redundantly with *lin-35* to control cell cycle exit in multiple postembryonic cell lineages of *C. elegans* (Fay et al., 2002). More recently, we identified a role for *lin-35* and a ubiquitin-conjugating enzyme, *ubc-18*, in the development of the anterior digestive tract (Fay et al., 2003). *lin-35; ubc-18* double mutants are defective at an early step in pharyngeal morphogenesis that involves a transformation in the orientation of a subset of pharyngeal cell precursors. This finding represents one of the first pieces of in vivo evidence demonstrating a role for Rb family proteins in organ morphogenesis and indicates that *lin-35* may have developmental functions that are not connected to cell cycle control. Other evidence to suggest a direct role for Rb family members in tissue morphogenesis includes recent work by Ruiz et al. (2003), demonstrating that the Rb-related proteins p107 and p130 function in the formation of hair follicles and incisors in mice. Consistent with this, microarray analyses indicate that both Rb and E2F participate in the regulation of a sizeable number of genes that are not connected to cell cycle control, including factors involved in cell adhesion, signal transduction, and pattern formation (Black et al., 2003; Dimova et al., 2003; Ishida et al., 2001; Markey et al., 2002; Muller et al., 2001; Russo et al., 2003; Vernell et al., 2003; Wells et al., 2003). Moreover, altered expression of E2F can disrupt embryonic patterning in both *C. elegans* and *Xenopus* through mechanisms that appear to be independent of cell cycle control (Page et al., 2001; Suzuki and Hemmati-Briuanlou, 2000).

Here, we report the identification of a synthetic genetic interaction between *lin-35* and mutations in the gene *pha-1*. Interestingly, *lin-35; pha-1* double mutants show defects in pharyngeal development that appear largely identical to those observed for *lin-35; ubc-18* double mutants. Moreover, we present genetic data suggesting that all three genes (*lin-35*, *pha-1*, and *ubc-18*) may function in parallel pathways to regulate a common molecular target.

Materials and methods

Strains and genetic methods

Maintenance, culturing, and genetic manipulations of *C. elegans* were carried out according to standard procedures at 16°C, 20°C, and 25°C, as indicated (Sulston and Hodgkin, 1988). Strains used in the phenotypic analysis include *lin-35(n745)*, WY119 [*lin-35; pha-1(fd1); kuEx119*], WY114 [*pha-1(fd1)*], WY128 [*lin-35; vab-7(e1562), pha-1(e2123); kuEx119*], WY115 [*lin-35; pha-1(fd1); pha-4::GFP; kuEx119*], WY116 [*lin-35; pha-1(fd1); myo-2::GFP; kuEx119*], WY117 [*lin-35; pha-1(fd1); ajm-1::GFP; kuEx119*], WY130 [*vab-7(e1562), pha-1(e2123); myo-2::GFP*], WY131 [*vab-7(e1562), pha-1(e2123); ajm-1::GFP*], WY132 [*vab-7(e1562), pha-1(e2123); pha-4::GFP-mem*], MH1384 (*ajm-1::GFP*), SM469 (*pha-4::GFP-NLS*), SM481 (*pha-4::GFP-mem*), PD4792 (*myo-2::GFP*), DP132 (*unc-119::GFP*), GE42 [*vab-7, pha-1(e2123)*], and GE24 [*pha-1(e2123)*]. The extrachromosomal array *kuEx119* expresses both wild-type *lin-35* as well as a ubiquitously expressed GFP reporter (*sur-5::GFP*; Fay et al., 2002).

To generate *lin-35; pha-1(fd1)/pha-1(e2123)* animals, we used the following two approaches: WY125 [*lin-35(n745); pha-1(fd1), dpy-18(e364); kuEx119*] animals were crossed to *lin-35* males and male cross-progeny were in turn mated to WY128 hermaphrodites. Cross-progeny animals of the correct genotype were identified as wild-type-appearing GFP+ hermaphrodites that produced wild-type, Dpy, and Vab progeny. We note that 42 of 43 F1 progeny that displayed the correct genotype generated strains that were dependent on the array (*kuEx119*) for viability. As an additional approach, we crossed *lin-35(n745)/+; pha-1(e2123), dpy-18(e364)* males to WY41 [*lin-35(n745); vab-7(e1562), pha-1(fd1); kuEx119*] hermaphrodites and identified the correct cross-progeny as wild-type GFP+ hermaphrodites that produced wild-type, Dpy, and Vab progeny and were dependent on the array (*kuEx119*) for viability.

Strains used to map *fd1* include WY64 [*lin-35(n745); vab-7(e1562), unc-71(e541)*], WY94 [*lin-35(n745); vab-7(e1562), fd1; unc-71(e541); kuEx119*], WY105 [*lin-35(n745)* back-crossed to CB4856 five times], and MH1797 [*lin-35(n745); unc-32(e189), vab-7(1562)*]. For three-point mapping with WY64, 26 of 29 Unc-non-Vab recombinants acquired the mutant *fd1* allele. SNP mapping was carried out using WY94 and WY105 to isolate Unc-

non-Vab recombinants of genotypes *lin-35; fd1, unc-71; kuEx119* and *lin-35; unc-71. fd1* was initially mapped to the left of SNP *eam62b02.s1@278,a,62; eam62b02.s1@278,a,62; and yy48e02.s1@180,a,62; and to the right of SNP yy44f01.s1@168,g,59*. Through sequencing of the CB4856 strain, we identified additional SNPs to place *fd1* to the right of the following polymorphism: a 10-bp insertion (CTAAAAAAT) in CB4856 between nucleotides 25,625/25,626 of sequencing contig Y48A6C. *fd1* was also placed to the left of the following polymorphisms in sequencing contig Y47D3A: G→T at position 35,344; C→T at 34,250; C→A at position 34,238; G→A at 32,935; and T→C at 32,854. This last polymorphism, along with the insertion at 25,625 of Y48A6C, formally defined the SNP mapping endpoints for *fd1*. This region spans 42,865 bp and contains five predicted open reading frames.

To test suppression of *lin-35; ubc-18* by *sup-36* and *sup-37, dpy-13, unc-24/+* and *dpy-11, unc-76/+* males were crossed into *lin-35; ubc-18, unc-32; kuEx119* hermaphrodites and cross-progeny males were further crossed to *sup-36* and *sup-37* hermaphrodites, respectively, to generate *lin-35/+; ubc-18, unc-32/+; sup-36/dpy-13, unc-24* and *lin-35/+; ubc-18, unc-32/+; sup-37/dpy-11, unc-76* hermaphrodites. Putative *lin-35; ubc-18, unc-32; sup-36* and *lin-35; ubc-18, unc-32; sup-37* animals were subsequently identified as Unc (*unc-32*) animals that failed to segregate Dpy Unc progeny (*dpy-13, unc-24* or *dpy-11, unc-76*) and expressed a Muv phenotype when placed on *lin-15a(RNAi) plates* (indicating that *lin-35* was homozygous). Finally, candidate strains were sequenced by PCR amplification to verify the presence of the homozygous *unc-18(ku354)* molecular lesion (Fay et al., 2003).

Other methods

pha-1 rescue

Rescue of *lin-35; pha-1(fd1)* synthetic lethality was obtained by injecting a mixture of plasmid pBX (Granato et al., 1994a,b), which contains the wild-type *pha-1* gene, and pRF4, which encodes a dominant roller gene (Mello and Fire, 1995), into WY119. Multiple non-GFP-expressing roller animals that no longer required the *kuEx119* array (containing *lin-35*-rescuing sequences) for viability were then identified in subsequent generations.

RNAi

RNAi was carried out according to standard methods (Fire et al., 1998; Fraser et al., 2000). Feeding vectors were constructed as previously described (Fay et al., 2002, 2003). For *pha-1* RNAi, a fragment spanning nucleotides 759–1424 of the *pha-1* cDNA was subcloned into the polylinker of pPD129.36. RNAi inactivation of *pha-1* (by feeding methods) substantially reduced, but did not abolish expres-

sion of the *pha-1::GFP* reporter, indicating that reduction of *pha-1* activity by this method is incomplete.

GFP reporter constructs

To express a functional PHA-1::GFP fusion protein, a genomic sequence containing approximately 2.9 kb of *pha-1* upstream regulatory sequences (from nucleotide position 28,395 of Y48A6C to the *pha-1* start codon at position 31,284) along with the *pha-1* genomic coding region (minus the C-terminal 8 aa) was fused in frame to GFP (at the C terminus of PHA-1). This construct (40 ng/μl) was injected into N2 animals along with pRF4 (100 ng/μl) and herring sperm DNA (30 ng/μl; as a carrier) to generate strains carrying stable extrachromosomal arrays. This expressed fusion construct was determined to be functional based on its ability to suppress the lethality of *pha-1(e2123)* mutants (at 25°C). Similar expression patterns were also observed using reporter constructs containing approximately 2.9 kb of upstream regulatory sequences together with genomic sequences encoding the first 137 aa of PHA-1 fused to a GFP containing a nuclear localization signal.

Computational analyses

The following Internet sites were used in our analysis of the PHA-1 peptide sequence:

http://www.ch.embnet.org/software/COILS_form.html
<http://www.paircoil.lcs.mit.edu/cgi-bin/paircoil>
<http://www.multicoil.lcs.mit.edu/cgi-bin/multicoil>
<http://www.2zip.molgen.mpg.de/index.html>
<http://www.psort.ims.u-tokyo.ac.jp/form2.html>

The following Internet sites were used in our analysis of the promoter region containing the mutation in *pha-1(fd1)* mutants:

<http://www.transfac.gbf.de/TRANSFAC/>
<http://www.cbil.upenn.edu/tess/>

Results

lin-35; fd1 double mutants are defective at pharyngeal development

In screens for mutations that show synthetic phenotypes with *lin-35/Rb* loss of function (LOF), we identified a single mutation (*fd1*) defining a genetic locus on the right arm of chromosome III (for details on screening methods, see Fay et al., 2002). Most *lin-35; fd1* double mutants arrested in early larval development, although a small percentage gradually matured into small sterile adults [Figs. 1A, B; Table 1; see *lin-35; pha-1(fd1)*]. Mutant adults frequently

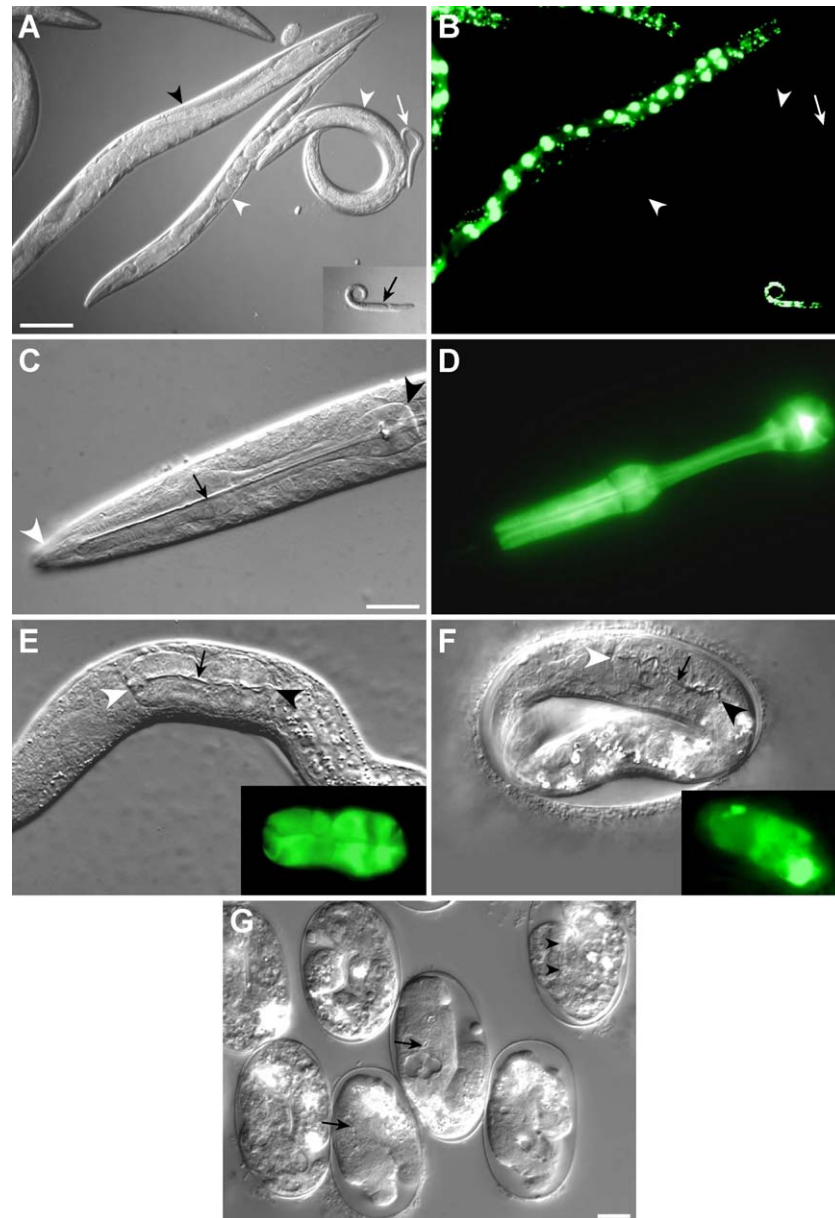


Fig. 1. Synthetic genetic interactions between *lin-35* and *pha-1*. DIC (A, C, E, F, G) and corresponding GFP fluorescence (B, D) images. (A) The large adult (black arrowhead) with GFP fluorescence is of genotype *lin-35; pha-1(fd1); kuEx119*. The small, growth-retarded adults (white arrowheads) and arrested larva (white arrow) are of genotype *lin-35; pha-1(fd1)*. Inset in A and B shows an arrested L1 larva (black arrow) of genotype *lin-35; pha-1(fd1); kuEx119* that was treated with *lin-35(RNAi)*. (C, D) Wild-type, (E) *lin-35; pha-1(fd1)*, and (F) *pha-1(e2123)* (at 25°C) L1 larvae expressing *myo-2::GFP* (insets E, F), which serves as a marker for pharyngeal muscle cell differentiation. Black and white arrowheads, posterior and anterior pharyngeal boundaries, respectively; black arrows, the pharyngeal lumen. Note the abnormal shape but clear expression of the *myo-2::GFP* reporter in the *lin-35; pha-1(fd1)* and *pha-1(e2123)* larvae. (G) Representative *pha-1(e2123)* (at 25°C) terminally arrested embryos showing morphogenetic defects in the pharynx as well as overall body plan. Black arrows indicate pharyngeal lumens. Note that the embryo in the upper right appears to have a ‘fully’ extended pharynx (arrowheads), but still shows strong defects in body morphogenesis, indicating that gross morphogenetic defects are not a secondary consequence of failed pharyngeal extension. Scale bars: A, 100 μ m for A, B; C, 10 μ m for C–F; G, 10 μ m for G.

had a clear or “starved” appearance, reminiscent of eating-defective mutants (Avery, 1993). An examination of larval-arrested *lin-35; fd1* mutants revealed that approximately 25% showed pharyngeal defects that were very similar to what had been observed for *lin-35; ubc-18* mutants (Figs. 1E, F; Table 1; Fay et al., 2003). The pharynges in these animals were markedly shortened as compared with wild

type (Figs. 1C, D) and did not form a functional connection to the mouth or buccal cavity (termed the Pun phenotype, for pharynx *unattached*). Upon hatching, such animals starved because of an inability to feed. Other larval-arrested double mutants showed more subtle defects such as irregular or indistinct pharyngeal contours (data not shown), which probably result in pharyngeal malfunction.

Table 1

Genetic interactions between *lin-35* and *pha-1*

	% Larval arrest ^a	% Pun	% Sterile	Average brood size
N2	<1 (many)	0 (n = 260)	<1 (many)	264 (±18) (n = 50) ^b
<i>lin-35</i> (n745)	1 (n = 268)	0 (n = 268)	4 (n = 100) ^b	98 (±43) (n = 10) ^b
<i>pha-1</i> (<i>fdl</i>)	9 (n = 504)	0 (n = 131)	0 (n = 30)	216 (±19) (n = 12)
<i>pha-1</i> (<i>e2123</i>) (16°C)	0 (n = 189)	0 (n = 189)	ND	ND
<i>lin-35</i> ; <i>pha-1</i> (<i>fdl</i>) ^c	93 (n = 91)	23 (n = 199)	100 (n = 20)	ND
<i>lin-35</i> ; <i>pha-1</i> (<i>e2123</i>) (16°C) ^c	100 (n = 148)	78 (n = 79)	ND	ND
<i>lin-35</i> ; <i>pha-1</i> (<i>e2123</i>)/ <i>pha-1</i> (<i>fdl</i>) (16°C) ^{c,d}	89 (n = 106)	12 (n = 92) ^c	90 (n = 30)	6 (n = 3)
<i>lin-35</i> ; <i>pha-1</i> (<i>fdl</i>)/+ ^f	0 (n = 113)	0 (n = 113)	60 (n = 20)	49 (±51) (n = 8)
<i>lin-35</i> ; <i>pha-1</i> (<i>e2123</i>)/+ (25°C) ^f	0 (n = 105)	0 (n = 105)	60 (n = 20)	36 (±40) (n = 8)
N2 <i>pha-1</i> (<i>RNAi</i>)	ND	0 (n = 129)	0 (n = 20)	ND
<i>lin-35</i> ; <i>pha-1</i> (<i>RNAi</i>)	ND	4 (n = 207)	100 (n = 20)	ND
<i>lin-35</i> ; <i>pha-1</i> (<i>fdl</i>); <i>pha-1</i> (<i>RNAi</i>)	ND	73 (n = 37)	ND	ND
N2 <i>lin-35</i> (<i>RNAi</i>)	ND	0 (n = 163)	ND	ND
<i>pha-1</i> (<i>fdl</i>); <i>lin-35</i> (<i>RNAi</i>)	76 (n = 177)	5 (n = 320)	97 (n = 30)	ND
<i>pha-1</i> (<i>e2123</i>); <i>lin-35</i> (<i>RNAi</i>) (16°C)	92 (n = 122)	75 (n = 63)	ND	ND

All experiments were conducted at 20°C unless otherwise indicated.

^a Animals either died as larvae or failed to reach maturity after 5 days.

^b Fay et al. (2002).

^c Double-mutant animals were derived from the self-progeny of *lin-35*; *pha-1*; *kuEx119* hermaphrodites. Progeny that failed to segregate the array (*kuEx119*–) were identified by their lack of GFP expression.

^d For details on the construction of this strain, see Materials and methods.

^e Non-Vab, non-Dpy larvae, derived from *lin-35*; *pha-1*(*fdl*), *dpy-18/vab-7*, *pha-1*(*e2123*) parents, were scored for the Pun phenotype.

^f Heterozygous animals were obtained by mating *lin-35* males to *lin-35*; *vab-7*, *pha-1*; *kuEx119* hermaphrodites and scoring the effects in the non-Vab *kuEx119*– progeny.

In contrast to the double mutants, *fdl* single mutants were largely healthy with normal pharynges and brood sizes that were similar to those of wild type (Table 1). We did, however, observe a low incidence of larval lethality in *fdl* single mutants (Table 1). These larvae had normal-appearing pharynges but arrested with a “fluid-filled” morphology that has been reported for many mutants, including hypomorphic alleles of genes comprising the Ras/MapK signaling pathway (Han and Sternberg, 1990; Yochem et al., 1997). This phenotype has been associated with defects in the excretory system, which functions in *C. elegans* osmoregulation (Nelson and Riddle, 1984). We note that this class of larval-arrested animals was not enhanced by the absence of *lin-35* function (data not shown) and could theoretically be due to a secondary mutation in a closely linked gene.

fdl defines a partial loss-of-function mutation in *pha-1*

fdl was genetically mapped using a combination of visible markers and single-nucleotide polymorphisms (SNPs) to an approximately 43-kb genomic region containing five predicted open reading frames (for details, see Materials and methods). Because cosmid-based genomic clones for use in transgenic rescue experiments were unavailable for this region, we took a reverse-genetics approach by testing the five candidate genes for synthetic lethality with *lin-35* using RNA-interference (RNAi). Only one of the five genes in this region, Y48A6C.5, showed a genetic interaction with *lin-35* by RNAi. Interestingly, this clone corresponds to *pha-1*, a gene previously implicated

in pharyngeal development (also see below). Although *pha-1*(*RNAi*) (by feeding methods) had no effect on wild-type animals (Gonczy et al., 2000; Kamath and Ahringer, 2003; and this study), presumably due to the inefficiency of the technique (also see methods), identically treated *lin-35* mutant animals either arrested as small larvae or progressed to become sterile adults (Table 1 and data not shown). Importantly, a low, but significant, percentage of arrested larvae showed pharyngeal defects including the Pun phenotype (Table 1). As further evidence that *fdl* defines an allele of *pha-1*, we were able to rescue the synthetic lethality of *lin-35*; *fdl* double mutants through the expression of wild-type *pha-1* from an extra-chromosomal array (see Materials and methods). Based on the above findings, as well as additional results presented below, we conclude that *fdl* represents a weak LOF mutation in *pha-1*.

To further examine the nature of the *fdl* allele, we reduced *pha-1* activity in *lin-35*; *pha-1*(*fdl*) double mutants through RNAi. As would be expected for a partial LOF mutation, RNAi of *pha-1* increased the severity of the phenotype beyond that of the untreated double-mutant strain (Table 1). In addition, we generated strains that were homozygous for *lin-35* but heterozygous for the *pha-1*(*fdl*) mutation. Although these animals did not display a Pun phenotype or arrest as larvae, we did observe an increase in sterility and a reduction in brood size, as compared with *lin-35* mutants alone (Table 1). This is likely attributable to a haploinsufficiency effect, a phenomenon we had also observed in *lin-35*; *ubc-18*/+ mutant animals (Fay et al., 2003).

To identify a genetic lesion, we first sequenced the coding region of *pha-1* in the *fdl* mutant background. Surprisingly, we failed to detect any differences from the established wild-type *pha-1* sequence, including the conserved splice-junction sites. To see if a regulatory element had been altered, we sequenced >3 kb upstream of the *pha-1* transcriptional start site, as well as the four introns and 3' UTR of the gene. Through this analysis, we identified a single lesion (C→T) occurring 156 bp upstream of the *pha-1* start methionine. This mutation was detected in six separate pooled-PCR reactions of *lin-35; pha-1(fdl)* and *pha-(fdl)* mutants, but was not present in the starting strain used to isolate the *fdl* mutation, *lin-35; kuEx119* (MH1461). The altered site [TATCC(C/T)TCCAG] does not correspond to consensus sequences for any known transcription factors (for details on the analysis tools used, see Materials and methods). Given the location of this mutation, a straightforward explanation is that the mutated site leads to a reduction in levels or delayed expression of the *pha-1* transcript. We note that the region covered by our sequencing analysis extends several hundred base pairs past the known poly-A signal of *pha-1* and includes >1 kb of upstream sequences that were previously shown to be unnecessary for complete rescue of the *pha-1* null phenotype (Granato et al., 1994a). Therefore, it is very unlikely that we have failed to identify any relevant mutations in a more distal regulatory element.

Previous work by Granato et al. (1994a) and Schnabel and Schnabel (1990) identified multiple mutations in *pha-1*, including the temperature-sensitive allele *e2123*. *e2123* leads to a strong LOF phenotype in *pha-1* (at the nonpermissive temperature of 25°C) and encodes an altered peptide containing a cysteine to tyrosine substitution at amino acid position 169. *pha-1(e2123)* mutants raised at

25°C arrest almost uniformly as embryos that contain abnormal (Pun) pharynges. In addition, these embryos often show defects in overall body morphogenesis, suggesting that *pha-1* may function in the development of other tissues (Fig. 1G; Schnabel and Schnabel, 1990). No obvious defects are visible in *pha-1(e2123)* mutants propagated at the permissive temperature of 16°C (Table 1; Schnabel and Schnabel, 1990). However, we found that *pha-1(e2123)* mutants grown at 16°C showed a strong synthetic phenotype with loss of *lin-35* function (either through mutation or RNAi; Table 1). Based on the percentages of Pun animals, the phenotype of *lin-35; pha-1(e2123)* mutants (at 16°C) appears to be more severe than that of *lin-35; pha-1(fdl)* animals at all temperatures (Table 1 and data not shown). Thus, the *fdl* allele of *pha-1* probably possesses more residual activity than the *e2123* allele at its permissive temperature of 16°C.

We found that strains heterozygous for both the *e2123* and *fdl* alleles of *pha-1* [*pha-1(e2123)/pha-1(fdl)*] were viable at all temperatures, consistent with *fdl* encoding a weak LOF mutation. We also used a variety of methods to generate *lin-35; pha-1(e2123)/pha-1(fdl)* animals (see Materials and methods) to assess the ability of these alleles to complement one another in the *lin-35* mutant background. As expected, *lin-35; pha-1(e2123)/pha-1(fdl)* mutants were nonviable and arrested primarily as larvae (Table 1). As a control, *lin-35; ubc-18(ku354)/pha-1(e2123)* animals were found to be uniformly viable (Table 2). These results further confirm that *fdl* is an allele of *pha-1*. Somewhat surprisingly, however, *lin-35; pha-1(e2123)/pha-1(fdl)* mutants showed a less severe phenotype (at both 16°C and 25°C) than either of the homozygous *lin-35; pha-1(fdl)* or *lin-35; pha-1(e2123)* (at 16°C) strains, based on the percentage of Pun larvae (Table 1 and data not shown).

Table 2
Genetic interactions between *pha-1* and *ubc-18*

	% Larval arrest ^a	% Pun	% Sterile	Average brood size
<i>ubc-18(ku354)</i> ^b	3 (n = 223)	0 (n = 101)	3 (n = 30)	9 (±28) (n = 14)
<i>ubc-18; pha-1(RNAi)</i>	ND	27 (n = 64)	ND	ND
<i>lin-35; ubc-18</i> ^b	84 (n = 192)	4 (n = 192)	72 (n = 30)	3 (±2) (n = 7)
<i>lin-35; ubc-18; pha-1(RNAi)</i>	ND	65 (n = 31)	ND	ND
N2 <i>ubc-18(RNAi)</i> ^b	0 (n = 100)	0 (n = 100)	0 (n = 30)	221 (±23) (n = 8)
<i>pha-1(fdl); ubc-18(RNAi)</i>	ND	0 (n = 285)	ND	ND
<i>pha-1(e2123); ubc-18(RNAi)</i> (16°C)	ND	77 (n = 62)	ND	ND
<i>lin-35; ubc-18(RNAi)</i> ^b	5 (n = 110)	0 (n = 255)	23 (n = 30)	55 (±34) (n = 10)
<i>lin-35; pha-1(fdl); ubc-18(RNAi)</i>	ND	66 (n = 111)	ND	ND
<i>lin-35; ubc-18; ubc-18(RNAi)</i> ^b	91 (n = 140)	40 (n = 174)	77 (n = 30)	2 (±2) (n = 7)
<i>lin-35; ubc-18(ku354)/pha-1(e2123)</i> (16°C) ^c	ND	0 (n = 167) ^d	5 (n = 20)	ND

All experiments were conducted at 20°C, unless otherwise indicated.

^a Animals either died as larvae or failed to reach maturity after 5 days.

^b Fay et al. (2003).

^c Animals of this genotype were generated by crossing *lin-35; ubc-18, unc-32/+* males to *lin-35; vab-7, pha-1(e2123); kuEx119* hermaphrodites. Cross-progeny of the correct genotype were identified by the presence of Unc and Vab progeny in the next generation as well as by the absence of GFP expression.

^d Non-Vab animals, derived from *lin-35; ubc-18, unc-32/vab-7, pha-1(e2123)* parents, were scored for the Pun phenotype as L1 larvae. Based on percentages, 2/3 of the non-Vab larvae should be of genotype *lin-35; ubc-18, unc-32/vab-7, pha-1(e2123)* whereas 1/3 should be of genotype *lin-35; ubc-18, unc-32*. The absence of any Pun larvae is not unexpected, given that the percentage of *lin-35; ubc-18* Pun animals is normally very low (see Table 2) and that expression of the Pun phenotype would be further diminished by the maternal rescue of *ubc-18* (Fay et al., 2003).

One possible explanation to account for this result is that the PHA-1 protein may function in vivo as a homodimer. Thus, in the mixed *lin-35; pha-1(e2123)/pha-1(fd1)* background, low levels of wild-type PHA-1 protein, generated by the *fd1* allele, may be able form functional dimers with the more abundant *e2123* PHA-1 protein product. This could lead to higher overall levels of PHA-1 dimer activity in the mixed allele strain than in homozygous *lin-35; pha-1(fd1)* or *lin-35; pha-1(e2123)* mutants.

lin-35; pha-1 mutants are defective at an early step in pharyngeal morphogenesis

To determine the underlying cause for the Pun phenotype, we analyzed three aspects of pharyngeal development in *lin-35; pha-1* double mutants: (1) the generation of pharyngeal precursor cells, (2) the ability of precursor cells to undergo terminal differentiation into multiple cell types, and (3) the morphogenetic events required to form the mature organ. Conceivably, defects in any of these processes could contribute to the observed phenotypes.

Specification of pharyngeal precursor cells is first initiated during the mid-proliferative phase of embryogenesis, approximately 150 min into development (Horner et al., 1998; Sulston et al., 1983). To detect pharyngeal precursor cells, we utilized a marker (*pha-4::GFP*) that is expressed in all cells destined to form the pharynx, as well as other cells comprising the digestive tract (e.g., intestinal, rectal, and arcade cells of the buccal cavity; Horner et al., 1998). More specifically, we counted *pha-4::GFP*⁺ cells in the head region of mutant and wild-type embryos at the 1.5-fold stage of embryogenesis, at which time pharyngeal elongation has been initiated in wild-type animals (Figs. 2A, B). Importantly, we scored only double-mutant embryos that had clearly failed to undergo pharyngeal elongation by this stage (Figs. 2C, D). We also note that based on the size, shape, and characteristic positions of intestinal cell nuclei, we were able to unambiguously exclude these cells from our counts.

lin-35; pha-1(fd1) double mutants showed a slight reduction in the average number of cells expressing the marker (95 ± 8 ; $n = 9$; range, 80–105) as compared with wild-type animals at this stage (100 ± 3 ; $n = 11$; range, 95–104; Figs. 2A–D; Fay et al., 2003). Of the nine mutant embryos analyzed, however, six contained 95 or more cells. This indicates that a large proportion (perhaps the majority) of mutant embryos contain indistinguishable numbers of pharyngeal cell precursors from wild type. Similar results were also observed in wild-type and *lin-35; pha-1(fd1)* mutant Pun larvae (Figs. 2E–H). Thus, differences in the number of pharyngeal precursor cells cannot account for the observed defects in our double mutants. We note that these results are nearly identical with our findings for *lin-35; ubc-18* double mutants (Fay et al., 2003). Furthermore, our results are consistent with earlier analyses of *pha-1* mutants, which detected no differences

in numbers of pharyngeal precursor cells in wild-type and *pha-1(e2123)* mutants at 25°C (Schnabel and Schnabel, 1990).

The Pun pharynges of *lin-35; pha-1(fd1)* double mutants, although abnormally shaped, displayed several characteristics that are consistent with normal tissue differentiation. These include the presence of a distinct pharyngeal lumen, suggesting the differentiation of epithelial cells (Figs. 1E, F). In addition, we have observed sustained rhythmic pumping, a property of the pharynx in wild-type animals, in many *lin-35; pha-1(fd1)* Pun larvae. This finding indicates the presence of functional muscle cells and may suggest some degree of proper neuronal connectivity. In further support of these results, we have observed strong expression of several GFP markers, indicating the presence of differentiated muscle (*myo-2::GFP*; Okkema et al., 1993), epithelium (*ajm-1::GFP*; Mohler et al., 1998), and neurons (*unc-119::GFP*; Maduro and Pilgrim, 1995) in the pharynges of *lin-35; pha-1(fd1)* Pun mutants (Figs. 1E, F and data not shown). We also note that we found no evidence indicating that the morphogenesis defects are the direct result of a delay in the timing of pharyngeal cell differentiation (data not shown). From these data, we conclude that the terminal differentiation of three pharyngeal cell types occurs in *lin-35; pha-1(fd1)* double mutants. However, based on our method of analysis, we cannot know that all cells within the classes examined underwent correct terminal differentiation.

We have previously shown that *lin-35; ubc-18* mutants are defective at an early step in pharyngeal morphogenesis (Fay et al., 2003), termed “reorientation” (Portereiko and Mango, 2001). At this time, a set of radially oriented anterior pharyngeal precursor cells undergoes a shift in their apical–basal polarity, such that their long axes become aligned with the dorsal ventral axis of the embryo (Fig. 3M). Using a membrane-localized GFP reporter that is expressed under the control of the *pha-4* promoter, we were able to follow this process in the double-mutant background. For technical reasons, these experiments were carried out using the *e2123* allele of *pha-1* (at 16°C) in combination with *lin-35(RNAi)*. Our findings indicate that, like *lin-35; ubc-18* mutants, the majority (11/16) of *lin-35; pha-1* mutants examined were at least partially defective at the reorientation step of pharyngeal morphogenesis (Figs. 3A–J). Interestingly, we found that *pha-1(e2123)* single-mutant embryos grown at 25°C were not defective at early stages of pharyngeal morphogenesis. Rather, these embryos underwent pharyngeal elongation in an apparently normal manner to form a transient attachment to the buccal cavity ($n > 100$; Figs. 3K, L). At some later stage, this connection is disrupted, leading to the Pun phenotype in *pha-1(e2123)* mutants (Schnabel and Schnabel, 1990; and data not shown). These results indicate that *pha-1* has both independent and overlapping functions with *lin-35* during pharyngeal development, and that early pharyngeal morphogenesis

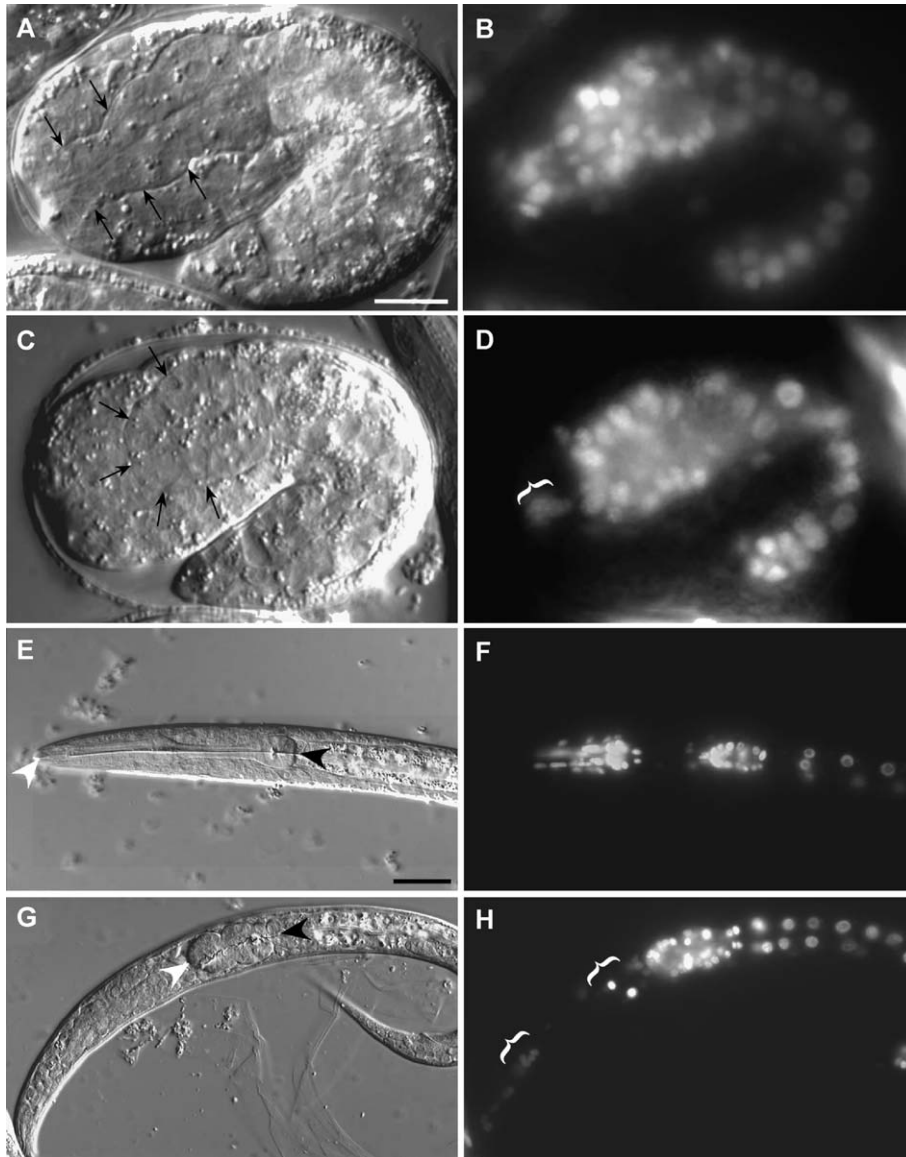


Fig. 2. *pha-4::GFP* expression in wild-type and *lin-35; pha-1* mutant animals. DIC (A, C, E, G) and corresponding *pha-4::GFP* fluorescence (B, D, F, H) images. (A–D) Approximately 1.5-fold-stage wild-type (A, B) and *lin-35; pha-1(fd1)* (C, D) embryos. Anterior is towards left and ventral is downwards. Arrows indicate the pharyngeal boundaries. Note the difference in pharyngeal shape between wild-type and *lin-35; pha-1(fd1)* embryos. For embryos in A and C, we detected 98 and 96 *pha-4::GFP*-expressing cells in the head region, respectively. The white bracket (D) demarcates several *GFP*-expressing arcade cells that have failed to integrate with the pharynx. Also showing strong *GFP* expression in both embryos are the round intestinal cell nuclei in the posterior region of the embryo. (E, F) Wild-type and (G, H) *lin-35; pha-1(fd1)* mutant (Pun) L1 larvae. Black and white arrowheads indicate the posterior and anterior pharyngeal boundaries. The white brackets in H indicate nonintegrated arcade cells. Scale bars: in A, 10 μ m for A–D; E, 10 μ m for E–H.

is controlled specifically by the overlapping activities of these gene products.

Differentiation in pha-1(e2123) mutants

Strong LOF mutations in *pha-1* were previously reported to interfere with the differentiation of multiple pharyngeal cell types (Granato et al., 1994a; Okkema et al., 1997; Schnabel and Schnabel, 1990). Three of the cell types examined (muscle, gland, and marginal cells) failed to express terminal differentiation markers based on antibody staining, and a fourth cell type (epithelium) was inferred to

be affected based on the absence (or grossly delayed appearance) of a pharyngeal lumen. Although these findings differed significantly from our own observations of *lin-35; pha-1(fd1)* double mutants, it was possible that our weak LOF allele of *pha-1(fd1)*, in combination with *lin-35* LOF, was producing a qualitatively different phenotype than strong LOF mutations in *pha-1*. Several observations, however, suggest that cell-type-specific differentiation may occur in *pha-1(e2123)* mutants to a greater extent than was previously thought. First, we observed a distinct pharyngeal lumen in 98% ($n = 110$) of newly hatched *pha-1(e2123)* larvae (at 25°C; as well as most late-stage embry-

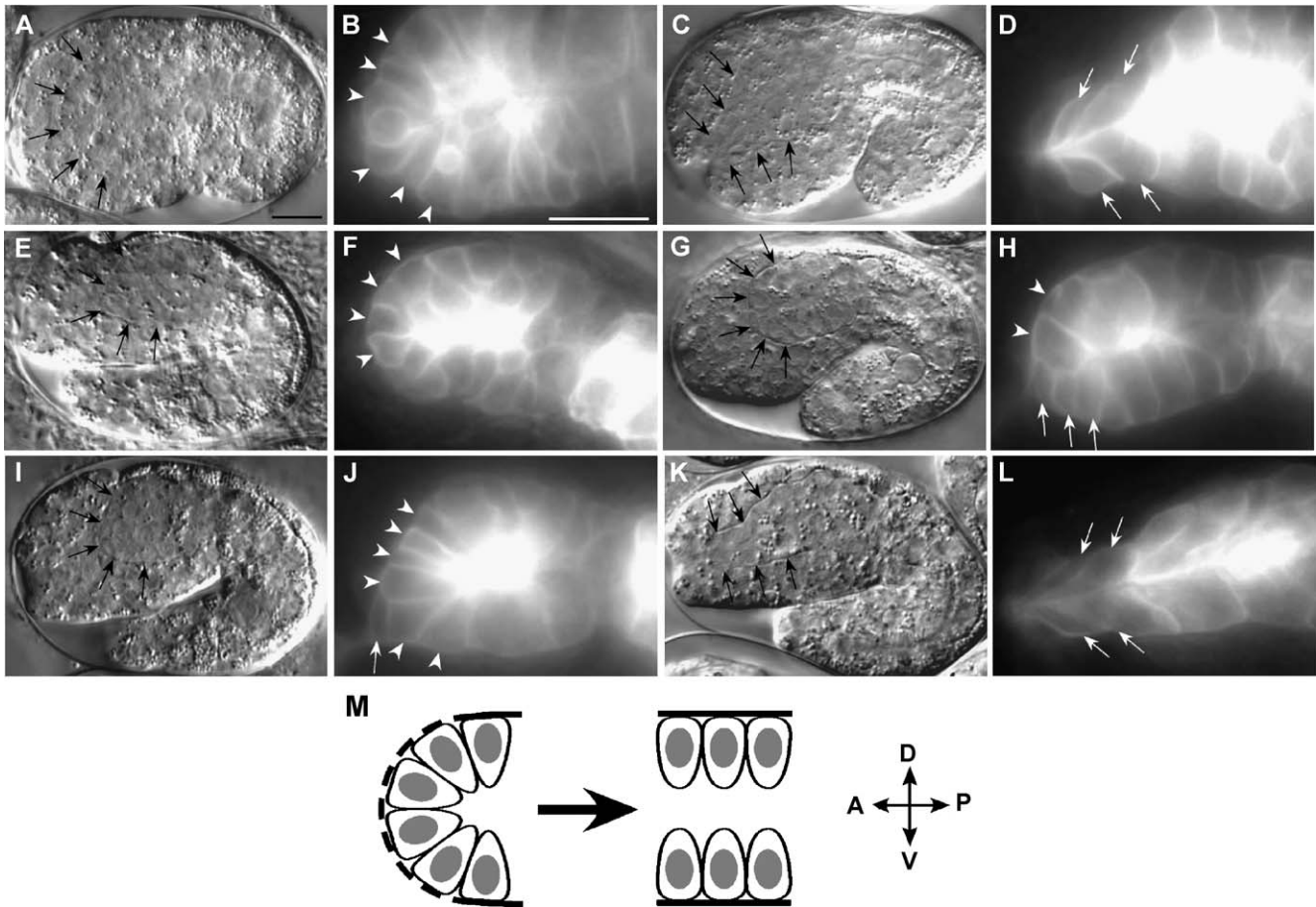


Fig. 3. Early pharyngeal morphogenesis in wild-type and mutant embryos. DIC (A, C, E, G, I, K) and corresponding fluorescence (B, D, F, H, J, L) images highlighting the shapes of pharyngeal cells. Black arrows, pharyngeal boundaries; white arrowheads, cells that have not undergone reorientation; white arrows, cells having completed or initiated reorientation. (A, B) A wild-type lima-bean-stage embryo before pharyngeal morphogenesis has initiated. Note the radially symmetric wedge-shaped leading-edge cells (arrowheads). (C, D) A wild-type 1.5-fold-stage embryo with early morphogenetic events completed. Note the shift in polarity of the leading-edge cells. (E–J) *pha-1(e2123); lin-35(RNAi)* 1.5- to 2-fold-stage embryos (at 16°C). Note the lack of pharyngeal extension and the presence of multiple leading-edge cells that have failed to undergo reorientation. (K, L) *pha-1(e2123)* single mutants at 25°C. Pharyngeal morphogenesis is apparently normal under these conditions. (M) Cell shape changes that normally occur during the reorientation step of pharyngeal morphogenesis. For further details, see text. Scale bars: in A, 10 μ m for A, C, E, G, I, K; in B, 10 μ m for B, D, F, H, J, L.

os; Figs. 1G, H and data not shown). Second, we observed robust expression of the *ajm-1::GFP* epithelial marker beginning at the comma stage of embryogenesis and persisting into adulthood (data not shown). Third, expression of the *myo-2::GFP* reporter was observed in nearly all (99%; $n = 64$) *pha-1(e2123)* mutants (at 25°C), beginning at about the 3-fold stage of embryogenesis (Figs. 1G, H and data not shown). Although the intensity of GFP staining in *pha-1(e2123)* mutants was somewhat reduced as compared with wild type, the onset of expression appeared to be identical. This result was surprising, as *pha-1(e2123)* mutants were initially reported to not express the protein product of *myo-2* (Granato et al., 1994a; Schnabel and Schnabel, 1990), based on staining patterns with MYO-2-specific monoclonal antibodies (Miller et al., 1983, 1986). It is possible, however, that some of these differences may be attributable to an increase in the sensitivity of our GFP reporter (*myo-2::GFP*) vs. antibody staining. In addition, it remains possible that

PHA-1 acts posttranscriptionally to promote the translation of *myo-2* mRNA, thereby accounting for the discrepancy between *myo-2* mRNA and protein levels.

pha-1 is widely expressed and is concentrated in the cytoplasm

To examine the expression pattern of *pha-1* during development, we generated strains that express a functional “full-length” PHA-1::GFP fusion protein under the regulatory control of the wild-type *pha-1* promoter (for details, see Materials and methods). Expression of the *pha-1* reporter was first detected at the approximately 100-cell stage in all somatic cells of the embryo (Figs. 4A, B). This pattern of widespread expression continued through later stages of embryonic development (Figs. 4C, D), diminishing somewhat in intensity by the time of hatching. Expression was also observed in early-larval-stage animals (Figs.

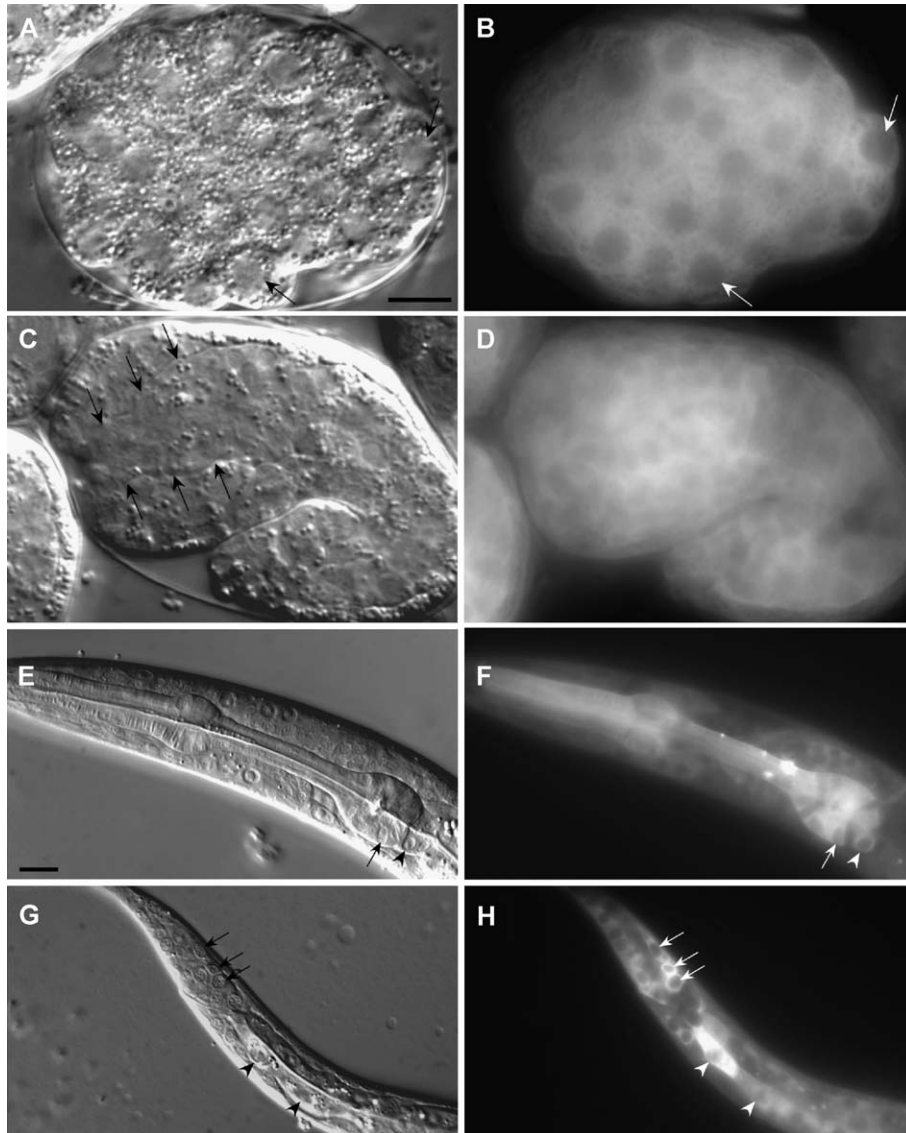


Fig. 4. Expression of *pha-1::GFP*. DIC (A, C, E, G) and corresponding fluorescence (B, D, F, H) images of a functional PHA-1::GFP fusion protein expressed under the control of the *pha-1* promoter. Note expression in essentially all cells at the approximately 100-cell (A, B) and late-comma (C, D) stages of embryonic development. Corresponding black and white arrows in panels A and B show the location of two nuclei. Note the lower level of nuclear vs. cytoplasmic expression. Black arrows in panel C indicate the pharyngeal borders. (E, F) Expression in the head region of an L2 larva. Corresponding black and white arrows, a GFP-expressing posterior pharyngeal muscle cell; black and white arrowheads, an anterior intestinal valve cell. (G, H) Expression in the tail of an L1 larva. Black and white arrows, GFP-expressing neuronal cells; black and white arrowheads, intestinal cells. Note that at all stages, expression is predominantly, if not exclusively, cytoplasmic. Scale bars: in A, 10 μ m for A–D; in E, 10 μ m for E–H.

4E–H) and was present but reduced in late-stage larvae and adults (data not shown). Strikingly, most if not all PHA-1::GFP fusion protein localized to the cytoplasm (Fig. 4). This was particularly apparent in larvae, where the contribution of nonspecific GFP fluorescence coming from layers outside of the central focal plane was minimized. In addition, we saw no evidence for any dynamic regulation of PHA-1 with respect to its subcellular localization. Although these findings do not rule out the possibility that some PHA-1 protein may normally be present in nuclei, they strongly suggest that PHA-1 resides primarily, if not exclusively, in the cytoplasmic compartment. Moreover,

although it was possible that the tagged fusion protein may have been mislocalized, either due to the presence of the C-terminal GFP extension, or simply through over-expression, the ability of the fusion protein to substitute functionally for wild-type PHA-1 suggests that it is localizing to the correct cellular compartment. We note that a previous report examining the expression pattern of *pha-1* using a (nonfunctional) *pha-1::lacZ* reporter detected transient expression in only pharyngeal precursor and body wall muscle cells (Granato et al., 1994a). Given that the regulatory regions used in these two reporter constructs were similar, these discrepancies may be attributable to

differences in the stability or sensitivity of β -galactosidase vs. GFP.

pha-1 was initially suggested to encode a transcription factor of the bZIP family (Granato et al., 1994a). This assignment was based on relatively weak sequence homologies between PHA-1 and the leucine-zipper and basic regions of seven other bZIP family members. However, as pointed out by the original authors, the spacing of these two regions in PHA-1 differed substantially from that of known bZIP proteins. Moreover, our detection of PHA-1::GFP in the cytoplasm would not be consistent with a role in transcriptional regulation. We therefore carried out a computational analysis on the predicted PHA-1 peptide to determine its probable molecular function. Our results strongly indicate that *pha-1* does not encode a bZIP transcription factor. PSORT, as well as several other Internet-based analysis programs (see Materials and methods), failed to detect three domains expected to be present in all bZIP factors including a coiled-coil domain, a leucine zipper, and a nuclear localization signal. In contrast, of the remaining 18 genes in the *C. elegans* genome with bZIP annotations, 17 are likely to contain coiled-coil domains (confidence values ≥ 0.6) based on these analysis tools (data not shown). Other classes of functional domains were not detected in our analysis of PHA-1, and the precise molecular function of this protein remains unclear. Nevertheless, our findings strongly indicate that *pha-1* does not encode a bZIP transcription factor and that its functions reside in the cytoplasm.

Genetic interactions between *pha-1* and *SynMuv* genes

We were interested in determining the degree to which the genetic interaction between *pha-1* and *lin-35* might be interchangeable with other *SynMuv* genes. Because RNAi inactivation of *lin-35* in the *pha-1(e2123)* mutant background (at 16°C) produced a much higher percentage of Pun larvae than *pha-1(fd1)* mutants (Table 3), we used the *e2123* allele (at 16°C) for all interaction tests. In summary, although the penetrance of the Pun phenotypes differed between the genes tested (possibly due to differential responses to RNAi treatment on the individual genes), a clear synthetic phenotype was observed for all class B *SynMuv* genes tested (Table 3). In contrast, the single class A gene tested, *lin-15a*, showed no sign of an interaction (Table 3). The class B genes tested included the histone deacetylase *hda-1* (Lu and Horvitz, 1998); the Mi2 homolog and NURD complex component *let-418* (Solari and Ahringer, 2000; von Zelewsky et al., 2000); the *C. elegans* RbAp46/48 homolog, *lin-53* (Lu and Horvitz, 1998); an E2F homolog, *efl-1* (Ceol and Horvitz, 2001); and two genes of unknown function, *lin-36* (Thomas and Horvitz, 1999) and *lin-37* (Boxem and van den Heuvel, 2002).

This spectrum of genetic interactions was nearly identical to that previously observed for *ubc-18* (Fay et al., 2003). However, in contrast to *pha-1*, we had not previously detected an interaction between *ubc-18* and *efl-1*. To exam-

Table 3
Genetic interactions with *SynMuv* genes

	% Pun ^a
N2 (wild type)	0 (many)
<i>pha-1(e2123)</i> ^b	0 (<i>n</i> = 189)
<i>lin-35(RNAi)</i> ^{c,d}	0 (<i>n</i> = 50)
<i>pha-1(fd1); lin-35(RNAi)</i> ^d	5 (<i>n</i> = 320)
<i>pha-1(e2123); lin-35(RNAi)</i> ^b	75 (<i>n</i> = 63)
<i>lin-37(RNAi)</i> ^{c,d}	0 (<i>n</i> = 62)
<i>pha-1(e2123); lin-37(RNAi)</i> ^b	42 (<i>n</i> = 104)
<i>lin-36(RNAi)</i> ^{c,d}	0 (<i>n</i> = 58)
<i>pha-1(e2123); lin-36(RNAi)</i> ^b	4 (<i>n</i> = 162)
<i>hda-1(RNAi)</i> ^{c,d,e}	1 (<i>n</i> = 60)
<i>pha-1(e2123); hda-1(RNAi)</i> ^b	13 (<i>n</i> = 67)
<i>let-418(RNAi)</i> ^{c,d,e}	1 (<i>n</i> = 313)
<i>pha-1(e2123); let-418(RNAi)</i> ^b	4 (<i>n</i> = 152)
<i>lin-53(RNAi)</i> ^{c,d,e}	0 (<i>n</i> = 73)
<i>pha-1(e2123); lin-53(RNAi)</i> ^b	50 (<i>n</i> = 6)
<i>efl-1(RNAi)</i> ^{c,d}	0 (<i>n</i> = 50)
<i>pha-1(e2123); efl-1(RNAi)</i> ^b	20 (<i>n</i> = 88)
<i>lin-15a(RNAi)</i> ^{c,d}	0 (<i>n</i> = 54)
<i>pha-1(e2123); lin-15a(RNAi)</i> ^b	0 (<i>n</i> = 182)
<i>lin-35; ubc-18(ku354)</i> ^{c,d}	4 (<i>n</i> = 192)
<i>lin-35; ubc-18(ku354); efl-1(RNAi)</i> ^d	57 (<i>n</i> = 95)

^a Includes both nonelongated and partially elongated pharynges.

^b Experiments were conducted at 16°C.

^c Fay et al. (2003).

^d Experiments were conducted at 20°C.

^e RNAi of these genes caused significant levels of sterility and embryonic lethality.

ine this further, we tested *ubc-18* for genetic interactions with *efl-1* using the *lin-35; ubc-18* double-mutant strain. Previous findings indicated that this strain would provide a more sensitized genetic background than *ubc-18(ku354)* single mutants [Fay et al., 2003; also compare the percentages of Pun animals in *lin-35; ubc-18(ku354)*, *lin-35; ubc-18(RNAi)*, and *lin-35; ubc-18(ku354); ubc-18(RNAi)* animals, Tables 1 and 3]. As shown in Table 3, inactivation of *efl-1* by RNAi dramatically increased the percentage of Pun animals in the *lin-35; ubc-18(ku354)* double-mutant background, indicating that, like *pha-1*, *efl-1* also shows genetic interactions with *ubc-18*.

PHA-1 and UBC-18 may regulate a common target

Given the striking similarities in their synthetic phenotypes with *lin-35*, as well as their matching sets of genetic interactions with other *SynMuv* genes, it seemed plausible that UBC-18 and PHA-1 might function as co-regulators of a common cellular target. One test of this hypothesis would be to inactivate both genes simultaneously. If UBC-18 and PHA-1 share overlapping functions, then a synthetic genetic interaction would be predicted. Because *pha-1* and *ubc-18* are located at similar positions on chromosome III (Fay et al., 2003; Granato et al., 1994a), we inactivated both genes using combinations of genetic mutations and RNAi (Table 2). In all cases but one, we observed a strong synthetic genetic interaction between *ubc-18* and *pha-1*, leading to a Pun phenotype. This included tests in both wild-type and

lin-35 backgrounds, as well as both the *fdl* and *e2123* alleles of *pha-1*. The single exception was *pha-1(fd1); ubc-18(RNAi)* animals, which probably failed to show an interaction because of the weak nature of the *fdl* allele and the incomplete effects of *ubc-18(RNAi)* (see above and Fay et al., 2003). We note that because we were limited to the use of partial LOF mutations for this study, it was not possible for us to determine whether UBC-18 and PHA-1 work in tandem or parallel pathways. Nevertheless, these results do indicate that PHA-1 and UBC-18 are likely to act on a common target.

As an additional test for functional convergence, we assayed the ability of two previously isolated extragenic suppressors of *pha-1* (*sup-36* and *sup-37*) to rescue the synthetic lethality of *lin-35; ubc-18* double mutants (Schnabel et al., 1991). *sup-36* and *sup-37* were previously shown to suppress the lethal phenotype of multiple strong LOF alleles in *pha-1*, indicating that they are very unlikely to be informational-type suppressors. Strikingly, both mutations were able to fully suppress the synthetic lethality of *lin-35; ubc-18* double mutants, as well as the lethality observed in *pha-1(e2123); lin-35(RNAi)* and in *pha-1(e2123); ubc-18(RNAi)* mutants (at 16°C). In contrast, neither mutation suppressed the expression of the SynMuv phenotype of *lin-35; lin-15a(RNAi)* animals, indicating that the suppressors are specific to the pharyngeal defect and not the *lin-35* pathway in general. Taken together, these results strongly support the model that PHA-1 and UBC-18 function as dual regulators of a single molecular process.

Discussion

A weak loss-of-function mutation in pha-1 reveals an underlying genetic redundancy

In this report, we have described a synthetic genetic interaction between LOF mutations in *lin-35* and *pha-1*. Although both *lin-35(n745)* and *pha-1(fd1)* single mutants are viable and generally appear indistinguishable from wild type, the large majority of double mutants arrest in early larval development with variable defects in pharyngeal development (Fig. 1; Table 1). However, whereas null mutations in *lin-35* show no obvious defects (Lu and Horvitz, 1998), strong LOF mutations in *pha-1* lead to a highly penetrant embryonic and larval lethality (Granato et al., 1994a; Schnabel and Schnabel, 1990). Thus, the genetic redundancy between *lin-35* and *pha-1* is revealed only through mutations or treatments (i.e., RNAi) that lead to a partial reduction in PHA-1 activity.

It is interesting to note that of the two mutations we have previously reported to show synthetic genetic interactions with *lin-35* [*fzr-1(ku298)* and *ubc-18(ku354)*], both resulted in partial LOF mutations in the affected genes (Fay et al., 2002, 2003). Moreover, in the case of *fzr-1*, RNAi injection experiments suggested that a null mutation in *fzr-*

1 may produce a sterile phenotype (Fay et al., 2002). Therefore, the detection of a genetic interaction between *lin-35* and *fzr-1*, like *pha-1*, may have been contingent upon our ability to isolate partial LOF mutations in this gene. These findings underscore the versatility and continued importance of this forward-genetic approach. They also indicate that functional redundancy is not merely a property associated with genes that cannot be mutated to an obvious visible phenotype, such as *lin-35*. The reality is more likely that most genes function in a variety of biological processes, only some of which can be discerned through the study of single mutations.

Cell proliferation, differentiation, or morphogenesis?

Several lines of evidence indicate that the morphogenetic defects observed in *lin-35; pha-1* and *lin-35; ubc-18* double mutants are not the direct result of cell cycle perturbations. One piece of evidence comes from our analyses of *pha-1* and *ubc-18* genetic interactions with class B SynMuv genes (Table 3 and Fay et al., 2003). Namely, both *pha-1* and *ubc-18* showed genetic interactions with many class B SynMuv genes that were previously shown not to play a role in cell cycle control (Boxem and van den Heuvel, 2002). At the same time, our current analysis did detect an interaction for both *pha-1* and *ubc-18* with E2F, a protein with well-characterized cell cycle functions. As discussed in the Introduction, however, E2F transcriptional targets include many genes that are not connected to cell cycle control (Dimova et al., 2003; Ishida et al., 2001; Muller et al., 2001), and there is precedent for non-cell-cycle functions of E2F in both *Xenopus* and *C. elegans* (Page et al., 2001; Suzuki and Hemmati-Brivanlou, 2000). In addition, neither cyclin-D nor *cdk4* is required for progression through embryonic cell cycles in *C. elegans* (Boxem and van den Heuvel, 2001; Park and Krause, 1999). Given that these two proteins are the principal upstream regulators of Rb in cell cycle regulation, these results indicate that in *C. elegans*, the Rb pathway is not controlling embryonic divisions. Finally, the phenotypes of *lin-35; ubc-18* and *lin-35; pha-1* double mutants are not suggestive of defects in cell cycle control (e.g., these mutants do not undergo supernumerary divisions).

We also obtained strong evidence that terminal differentiation of multiple pharyngeal cell types takes place in both *lin-35; pha-1* and *lin-35; ubc-18* double-mutant animals (this study and Fay et al., 2003). In addition, through our analysis of the strong LOF mutation, *pha-1(e2123)*, we found that differentiation of pharyngeal epithelial and muscle cells may occur to a greater extent than earlier reports had suggested (Figs. 1G, H and data not shown). However, we note that we did find evidence for a subtle but reproducible delay in the timing of differentiation of pharyngeal epithelial cells in both *lin-35* and *pha-1(e2123)* (at 25°C) single mutants (based on the *ajm-1::GFP* marker; data not shown). However, given that neither of these single mutants is defective at early steps of pharyngeal morphogenesis, it is

unclear as to how this delay might be relevant to the observed defects in the double mutants.

Complementary pathways controlling organ morphogenesis in *C. elegans*

We have now shown that three genes, *lin-35*, *ubc-18*, and *pha-1*, function in a partially redundant manner to control pharyngeal morphogenesis during *C. elegans* embryonic development (Tables 1 and 2; Fay et al., 2003). Four pieces of evidence indicate that the activities of these genes converge on a common cellular target (or set of targets). (1) The developmental defects of *lin-35; ubc-18* and *lin-35; pha-1* double mutants are essentially indistinguishable. (2) *ubc-18* and *pha-1* are identical with respect to their genetic interactions with SynMuv genes. (3) *ubc-18* and *pha-1* are themselves synthetically lethal and display a Pun phenotype that appears identical to that of *lin-35; ubc-18* and *lin-35; pha-1* double mutants (Table 2 and data not shown). (4) Mutations that can suppress the lethality of strong LOF mutations in *pha-1* also suppress the lethality of *lin-35; ubc-18* double mutants. It is tempting to speculate that these suppressor mutations may in fact directly affect the mutual target(s) of LIN-35, UBC-18, and PHA-1 or may occur in genes that are required for the activation of a common target (Fig. 5 and also see below).

We have previously suggested a model to explain the functional redundancy of *lin-35* and *ubc-18* (Fay et al., 2003). The model is based on our current understanding of the principal functions carried out by Rb family proteins and ubiquitin-conjugating enzymes. Namely, LIN-35, a presumed negative regulator of transcription, and UBC-18, a component of the ubiquitin-mediated proteolysis pathway, would share in common one or more cellular targets (Fig. 5A). In the absence of either LIN-35 or UBC-18 activity (but not both), sufficient negative regulation of the mutual target could be brought about through either pathway acting alone. In the double mutant, however, two principal means of regulation have now been abolished, and the activity of the target would go largely unchecked. More specifically, since both LIN-35 and UBC-18 would be expected to affect the overall abundance of the target protein (vs. its inherent activity), the simultaneous loss of both pathways would lead to the overexpression of the shared target. This model is especially attractive since we have previously obtained evidence that LIN-35 and FZR-1, a conserved component of the anaphase-promoting complex (a multisubunit ubiquitin ligase), cooperate to negatively regulate the levels of G1 cyclins (Fay et al., 2002).

Where PHA-1 may fit into this process is currently unclear. The initial characterization of *pha-1* identified a weak homology to bZIP transcription factors. However, based on the expression pattern of a functional PHA-1::GFP fusion protein (Fig. 4), as well as our computational analysis of the peptide sequence (see Results), we

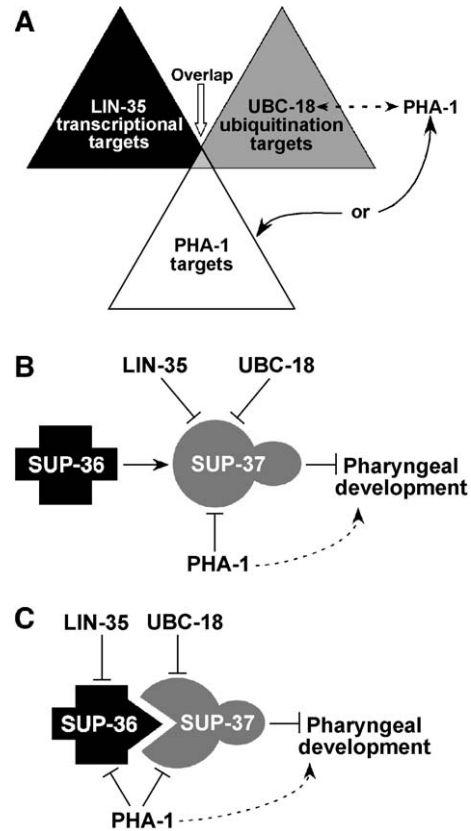


Fig. 5. Models of functional redundancy. (A) Modified Venn diagram indicating the hypothesized independent and overlapping targets of LIN-35, UBC-18, and PHA-1. In the case of LIN-35 and UBC-18, targets are presumed to be regulated through transcriptional inhibition and ubiquitin-mediated proteolysis, respectively. The biochemical function of PHA-1 is not known. Genetic analyses indicate that PHA-1 could act either in a proteolytic pathway with UBC-18 (indicated by the dashed double-headed arrow) or through an independent mechanism. Note that the equal size of the triangles is not meant to suggest that LIN-35, UBC-18, and PHA-1 regulate similar numbers of independent targets. (B, C) Two potential regulatory circuits to account for the observed genetic interactions of *lin-35*, *ubc-18*, *pha-1*, *sup-36*, and *sup-37*. In panel B, LIN-35, UBC-18, and PHA-1 converge on a single regulatory target (SUP-37), which if present at high levels inhibits pharyngeal morphogenesis. In this scenario, SUP-36 functions as an upstream activator of SUP-37 and therefore loss of *sup-36* can suppress overexpression of SUP-37. In panel C, LIN-35 and UBC-18 act on distinct subunits of a molecular complex (SUP-36-SUP-37), whereas PHA-1 acts on both subunits. In this scenario, loss of LIN-35 and UBC-18 function would result in the moderate overexpression of both subunits. Given the lethal phenotype of *pha-1* strong LOF mutations, PHA-1 is also shown in both panels to affect pharyngeal development/morphogenesis through an independent pathway (dashed line). For additional details, see text.

believe that this is unlikely to be the case. Moreover, because PHA-1 does not contain any known motifs to suggest a biochemical function, we can only speculate at present as to how PHA-1 may intersect with the LIN-35 and UBC-18 pathways to control pharyngeal morphogenesis. Our genetic analysis (Table 2) currently supports a model whereby PHA-1 could act either in the same pathway as UBC-18 or through some independent mechanism (Fig. 5A).

As mentioned above, two obvious candidates for regulation by LIN-35, UBC-18, (and PHA-1) are the suppressors, SUP-36 and SUP-37. The rationale is that hypomorphic mutations in the target would be predicted to compensate for an overabundance (or hyperactivity) of the protein product. Alternatively, suppression could occur if the mutation affected an important binding partner of the target (e.g., if the target functions as a heterodimer) or an upstream activator of the target (Figs. 5B, C). It is also worth pointing out that LIN-35 and UBC-18 could be acting independently on different members of a heterodimeric protein complex, such that the observed synergy results from the simultaneous mis-expression of both complex subunits (Fig. 5C). As to the molecular nature of these targets, we can only speculate at present. One possibility, however, is suggested by a recent paper describing the role of the ubiquitin ligase, Smurf1, in the regulation of cell polarity in mammals. Specifically, Smurf1 is recruited to the leading-edge projections of migrating cells by atypical protein kinase C and CDC42-PAR6, where it regulates the actin cytoskeleton through the inhibition of the RhoA GTPase (Wang et al., 2003). Thus, signaling molecules and other factors that control cell polarity are obvious candidates as targets.

Additional studies will be necessary to determine the function of PHA-1 and to understand how the activities of PHA-1, LIN-35, and UBC-18 are integrated at the molecular level. These studies will lead to a greater understanding of Rb family functions in development and will also provide further insight into the complexities of redundant cellular mechanisms.

Acknowledgments

We would like to thank the *C. elegans* Genetics Consortium, Jeff Hardin, Andy Fire, and David Pilgrim for strains and constructs. We thank Amy Fluet for a critical reading of the manuscript. We especially thank Mary Ellen Domeier for her work in constructing the *pha-1::GFP* expression constructs and strains. This work was supported by a research grant from the American Cancer Society, R01 GM56264, and by the University of Wyoming.

References

- Avery, L., 1993. The genetics of feeding in *Caenorhabditis elegans*. *Genetics* 133, 897–917.
- Black, E.P., Huang, E., Dressman, H., Rempel, R., Laakso, N., Asa, S.L., Ishida, S., West, M., Nevins, J.R., 2003. Distinct gene expression phenotypes of cells lacking Rb and Rb family members. *Cancer Res.* 63, 3716–3723.
- Boxem, M., van den Heuvel, S., 2001. lin-35 Rb and cki-1 Cip/Kip cooperate in developmental regulation of G1 progression in *C. elegans*. *Development* 128, 4349–4359.
- Boxem, M., van den Heuvel, S., 2002. *C. elegans* class B synthetic multivulva genes act in G(1) regulation. *Curr. Biol.* 12, 906–911.
- Brehm, A., Miska, E.A., McCance, D.J., Reid, J.L., Bannister, A.J., Kouzarides, T., 1998. Retinoblastoma protein recruits histone deacetylase to repress transcription. *Nature* 391, 597–601.
- Ceol, C.J., Horvitz, H.R., 2001. dpl-1 DP and efl-1 E2F act with lin-35 Rb to antagonize Ras signaling in *C. elegans* vulval development. *Mol. Cell* 7, 461–473.
- Couteau, F., Guerry, F., Muller, F., Palladino, F., 2002. A heterochromatin protein 1 homologue in *Caenorhabditis elegans* acts in germline and vulval development. *EMBO Rep.* 3, 235–241.
- Dahiya, A., Wong, S., Gonzalo, S., Gavin, M., Dean, D.C., 2001. Linking the Rb and polycomb pathways. *Mol. Cell* 8, 557–569.
- DeGregori, J., Kowalik, T., Nevins, J.R., 1995. Cellular targets for activation by the E2F1 transcription factor include DNA synthesis- and G1/S-regulatory genes. *Mol. Cell. Biol.* 15, 4215–4224.
- Dimova, D.K., Stevaux, O., Frolow, M.V., Dyson, N.J., 2003. Cell cycle-dependent and cell cycle-independent control of transcription by the *Drosophila* E2F/RB pathway. *Genes Dev.* 17, 2308–2320.
- Dou, Q.P., Zhao, S., Levin, A.H., Wang, J., Helin, K., Pardee, A.B., 1994. G1/S-regulated E2F-containing protein complexes bind to the mouse thymidine kinase gene promoter. *J. Biol. Chem.* 269, 1306–1313.
- Dunaief, J.L., Strober, B.E., Guha, S., Khavari, P.A., Alin, K., Luban, J., Begemann, M., Crabtree, G.R., Goff, S.P., 1994. The retinoblastoma protein and BRG1 form a complex and cooperate to induce cell cycle arrest. *Cell* 79, 119–130.
- Fay, D.S., Han, M., 2000. The synthetic multivulval genes of *C. elegans*: functional redundancy, Ras-antagonism, and cell fate determination. *Genesis* 26, 279–284.
- Fay, D.S., Keenan, S., Han, M., 2002. *fzr-1* and *lin-35/Rb* function redundantly to control cell proliferation in *C. elegans* as revealed by a non-biased synthetic screen. *Genes Dev.* 16, 503–517.
- Fay, D.S., Large, E., Han, M., Darland, M., 2003. *lin-35/Rb* and *ubc-18*, an E2 ubiquitin-conjugating enzyme, function redundantly to control pharyngeal morphogenesis in *C. elegans*. *Development* 130, 3319–3330.
- Ferguson, E.L., Horvitz, H.R., 1989. The multivulva phenotype of certain *Caenorhabditis elegans* mutants results from defects in two functionally redundant pathways. *Genetics* 123, 109–121.
- Fire, A., Xu, S., Montgomery, M.K., Kostas, S.A., Driver, S.E., Mello, C.C., 1998. Potent and specific genetic interference by double-stranded RNA in *Caenorhabditis elegans* [see comments]. *Nature* 391, 806–811.
- Fraser, A.G., Kamath, R.S., Zipperlen, P., Martinez-Campos, M., Souhrmann, M., Ahringer, J., 2000. Functional genomic analysis of *C. elegans* chromosome I by systematic RNA interference. *Nature* 408, 325–330.
- Gonczy, P., Echeverri, C., Oegema, K., Coulson, A., Jones, S.J., Copley, R.R., Duperon, J., Oegema, J., Brehm, M., Cassin, E., Hannak, E., Kirkham, M., Pichler, S., Flohrs, K., Goessen, A., Leidel, S., Alleaume, A.M., Martin, C., Ozlu, N., Bork, P., Hyman, A.A., 2000. Functional genomic analysis of cell division in *C. elegans* using RNAi of genes on chromosome III. *Nature* 408, 331–336.
- Granato, M., Schnabel, H., Schnabel, R., 1994a. Genesis of an organ: molecular analysis of the *pha-1* gene. *Development* 120, 3005–3017.
- Granato, M., Schnabel, H., Schnabel, R., 1994b. *pha-1*, a selectable marker for gene transfer in *C. elegans*. *Nucleic Acids Res.* 22, 1762–1763.
- Han, M., Sternberg, P.W., 1990. *let-60*, a gene that specifies cell fates during *C. elegans* vulval induction, encodes a ras protein. *Cell* 63, 921–931.
- Harbour, J.W., Dean, D.C., 2000. The Rb/E2F pathway: expanding roles and emerging paradigms. *Genes Dev.* 14, 2393–2409.
- Hodgkin, J., 2001. What does a worm want with 20,000 genes? *Genome Biol.* 2 (COMMENT2008).
- Horner, M.A., Quintin, S., Domeier, M.E., Kimble, J., Labouesse, M., Mango, S.E., 1998. *pha-4*, an HNF-3 homolog, specifies pharyngeal organ identity in *Caenorhabditis elegans*. *Genes Dev.* 12, 1947–1952.
- Ishida, S., Huang, E., Zuzan, H., Spang, R., Leone, G., West, M., Nevins, J.R., 2001. Role for E2F in control of both DNA replication and mitotic functions as revealed from DNA microarray analysis. *Mol. Cell. Biol.* 21, 4684–4699.
- Kaelin Jr., W.G., 1999. Functions of the retinoblastoma protein. *BioEssays* 21, 950–958.

- Kamath, R.S., Ahringer, J., 2003. Genome-wide RNAi screening in *Caenorhabditis elegans*. *Methods* 30, 313–321.
- Lu, X., Horvitz, H.R., 1998. *lin-35* and *lin-53*, two genes that antagonize a *C. elegans* Ras pathway, encode proteins similar to Rb and its binding protein RbAp48. *Cell* 95, 981–991.
- Luo, R.X., Postigo, A.A., Dean, D.C., 1998. Rb interacts with histone deacetylase to repress transcription. *Cell* 92, 463–473.
- Maduro, M., Pilgrim, D., 1995. Identification and cloning of *unc-119*, a gene expressed in the *Caenorhabditis elegans* nervous system. *Genetics* 141, 977–988.
- Magnaghi-Jaulin, L., Groisman, R., Naguibneva, I., Robin, P., Lorain, S., Le Villain, J.P., Troalen, F., Trouche, D., Harel-Bellan, A., 1998. Retinoblastoma protein represses transcription by recruiting a histone deacetylase. *Nature* 391, 601–605.
- Markey, M.P., Angus, S.P., Strobeck, M.W., Williams, S.L., Gunawardena, R.W., Aronow, B.J., Knudsen, E.S., 2002. Unbiased analysis of RB-mediated transcriptional repression identifies novel targets and distinctions from E2F action. *Cancer Res.* 62, 6587–6597.
- Mello, C., Fire, A., 1995. DNA transformation. *Methods Cell Biol.* 48, 451–482.
- Miller III, D.M., Ortiz, I., Berliner, G.C., Epstein, H.F. 1983. Differential localization of two myosins within nematode thick filaments. *Cell* 34, 477–490.
- Miller, D.M., Stockdale, F.E., Kam, J., 1986. Immunological identification of the genes encoding the four myosin heavy chain isoforms of *Caenorhabditis elegans*. *Proc. Natl. Acad. Sci. U. S. A.* 83, 2305–2309.
- Mohler, W.A., Simske, J.S., Williams-Masson, E.M., Hardin, J.D., White, J.G., 1998. Dynamics and ultrastructure of developmental cell fusions in the *Caenorhabditis elegans* hypodermis. *Curr. Biol.* 8, 1087–1090.
- Morris, E.J., Dyson, N.J., 2001. Retinoblastoma protein partners. *Adv. Cancer Res.* 82, 1–54.
- Muller, H., Bracken, A.P., Vernell, R., Moroni, M.C., Christians, F., Grassilli, E., Prosperini, E., Vigo, E., Oliner, J.D., Helin, K., 2001. E2Fs regulate the expression of genes involved in differentiation, development, proliferation, and apoptosis. *Genes Dev.* 15, 267–285.
- Narita, M., Nunez, S., Heard, E., Lin, A.W., Hearn, S.A., Spector, D.L., Hannon, G.J., Lowe, S.W., 2003. Rb-mediated heterochromatin formation and silencing of E2F target genes during cellular senescence. *Cell* 113, 703–716.
- Nelson, F.K., Riddle, D.L., 1984. Functional study of the *Caenorhabditis elegans* secretory–excretory system using laser microsurgery. *J. Exp. Zool.* 231, 45–56.
- Nielsen, S.J., Schneider, R., Bauer, U.M., Bannister, A.J., Morrison, A., O’Carroll, D., Firestein, R., Cleary, M., Jenuwein, T., Herrera, R.E., Kouzarides, T., 2001. Rb targets histone H3 methylation and HP1 to promoters. *Nature* 412, 561–565.
- Okkema, P.G., Harrison, S.W., Plunger, V., Aryana, A., Fire, A., 1993. Sequence requirements for myosin gene expression and regulation in *Caenorhabditis elegans*. *Genetics* 135, 385–404.
- Okkema, P.G., Ha, E., Haun, C., Chen, W., Fire, A., 1997. The *Caenorhabditis elegans* NK-2 homeobox gene *ceh-22* activates pharyngeal muscle gene expression in combination with *pha-1* and is required for normal pharyngeal development. *Development* 124, 3965–3973.
- Page, B.D., Guedes, S., Waring, D., Priess, J.R., 2001. The *C. elegans* E2F- and DP-related proteins are required for embryonic asymmetry and negatively regulate Ras/MAPK signaling. *Mol. Cell* 7, 451–460.
- Park, M., Krause, M.W., 1999. Regulation of postembryonic G(1) cell cycle progression in *Caenorhabditis elegans* by a cyclin D/CDK-like complex. *Development* 126, 4849–4860.
- Portereiko, M.F., Mango, S.E., 2001. Early morphogenesis of the *Caenorhabditis elegans* pharynx. *Dev. Biol.* 233, 482–494.
- Ruiz, S., Segrelles, C., Bravo, A., Santos, M., Perez, P., Leis, H., Jorcano, J.L., Paramio, J.M., 2003. Abnormal epidermal differentiation and impaired epithelial–mesenchymal tissue interactions in mice lacking the retinoblastoma relatives p107 and p130. *Development* 130, 2341–2353.
- Russo, G., Claudio, P.P., Fu, Y., Stiegler, P., Yu, Z., Macaluso, M., Giordano, A., 2003. pRB2/p130 target genes in non-small lung cancer cells identified by microarray analysis. *Oncogene* 22, 6959–6969.
- Schnabel, H., Schnabel, R., 1990. An organ-specific differentiation gene, *pha-1*, from *Caenorhabditis elegans*. *Science* 250, 686–688.
- Schnabel, H., Bauer, G., Schnabel, R., 1991. Suppressors of the organ-specific differentiation gene *pha-1* of *Caenorhabditis elegans*. *Genetics* 129, 69–77.
- Smith, V., Chou, K.N., Lashkari, D., Botstein, D., Brown, P.O., 1996. Functional analysis of the genes of yeast chromosome V by genetic footprinting. *Science* 274, 2069–2074.
- Solari, F., Ahringer, J., 2000. NURD-complex genes antagonise Ras-induced vulval development in *Caenorhabditis elegans*. *Curr. Biol.* 10, 223–226.
- Strober, B.E., Dunaief, J.L., Guha, Goff, S.P., 1996. Functional interactions between the hBRM/hBRG1 transcriptional activators and the pRB family of proteins. *Mol. Cell Biol.* 16, 1576–1583.
- Sulston, J.E., Hodgkin, J., 1988. Methods. In: Wood, W.B., Community of *C. elegans* Researchers (Eds.), *The nematode Caenorhabditis elegans*. Cold Spring Harbor Laboratory Press, Cold Spring Harbor, New York, pp. 587–606.
- Sulston, J.E., Schierenberg, E., White, J.G., Thomson, J.N., 1983. The embryonic cell lineage of the nematode *Caenorhabditis elegans*. *Dev. Biol.* 100, 64–119.
- Suzuki, A., Hemmati-Brivanlou, A., 2000. *Xenopus* embryonic E2F is required for the formation of ventral and posterior cell fates during early embryogenesis. *Mol. Cell* 5, 217–229.
- Thomas, J.H., Horvitz, H.R., 1999. The *C. elegans* gene *lin-36* acts cell autonomously in the *lin-35* Rb pathway. *Development* 126, 3449–3459.
- Tong, A.H., Lesage, G., Bader, G.D., Ding, H., Xu, H., Xin, X., Young, J., Berriz, G.F., Brost, R.L., Chang, M., Chen, Y., Cheng, X., Chua, G., Friesen, H., Goldberg, D.S., Haynes, J., Humphries, C., He, G., Husein, S., Ke, L., Krogan, N., Li, Z., Levinson, J.N., Lu, H., Menard, P., Munyana, C., Parsons, A.B., Ryan, O., Tonikian, R., Roberts, T., Sdicu, A.M., Shapiro, J., Sheikh, B., Suter, B., Wong, S.L., Zhang, L.V., Zhu, H., Burd, C.G., Munro, S., Sander, C., Rine, J., Greenblatt, J., Peter, M., Bretschke, A., Bell, G., Roth, F.P., Brown, G.W., Andrews, B., Bussey, H., Boone, C., 2004. Global mapping of the yeast genetic interaction network. *Science* 303, 808–813.
- Vernell, R., Helin, K., Muller, H., 2003. Identification of target genes of the p16INK4A-pRB-E2F pathway. *J. Biol. Chem.* 278, 46124–46137.
- von Zelewsky, T., Palladino, F., Brunschwig, K., Tobler, H., Hajnal, A., Muller, F., 2000. The *C. elegans* Mi-2 chromatin-remodelling proteins function in vulval cell fate determination. *Development* 127, 5277–5284.
- Wang, H.R., Zhang, Y., Ozdamar, B., Ogunjimi, A.A., Alexandrova, E., Thomsen, G.H., Wrana, J.L., 2003. Regulation of cell polarity and protrusion formation by targeting RhoA for degradation. *Science* 302, 1775–1779.
- Wells, J., Yan, P.S., Cechvala, M., Huang, T., Farnham, P.J., 2003. Identification of novel pRb binding sites using CpG microarrays suggests that E2F recruits pRb to specific genomic sites during S phase. *Oncogene* 22, 1445–1460.
- Winzler, E.A., Shoemaker, D.D., Astromoff, A., Liang, H., Anderson, K., Andre, B., Bangham, R., Benito, R., Boeke, J.D., Bussey, H., Chu, A.M., Connelly, C., Davis, K., Dietrich, F., Dow, S.W., El Bakkoury, M., Foury, F., Friend, S.H., Gentalen, E., Giaever, G., Hegemann, J.H., Jones, T., Laub, M., Liao, H., Davis, R.W., et al., 1999. Functional characterization of the *S. cerevisiae* genome by gene deletion and parallel analysis. *Science* 285, 901–906.
- Yochem, J., Sundaram, M., Han, M., 1997. Ras is required for a limited number of cell fates and not for general proliferation in *Caenorhabditis elegans*. *Mol. Cell Biol.* 17, 2716–2722.
- Zhang, H.S., Gavin, M., Dahiya, A., Postigo, A.A., Ma, D., Luo, R.X., Harbour, J.W., Dean, D.C., 2000. Exit from G1 and S phase of the cell cycle is regulated by repressor complexes containing HDAC-Rb-hSWI/SNF and Rb-hSWI/SNF. *Cell* 101, 79–89.